International Journal of ChemTech Research
CODEN (USA): IJCRGG ISSN: 0974-4290
Vol.7, No.3, pp 1474-1480, 2014-2015

ICONN 2015 [4th - 6th Feb 2015]
International Conference on Nanoscience and Nanotechnology-2015
SRM University, Chennai, India

Structural and optical properties of co-doped (Fe, Al) SnO_2 nanoparticles

P. Venkateswara Reddy[1], S. Venkatramana Reddy[1]* and B. Sankara Reddy[1]

[1]Dept of Physics, Sri Venkateswara University, Tirupati, A.P., India.

Abstract : Pure and co-doped SnO_2 with Al and Fe nanoparticles have been successfully synthesized by chemical co-precipitation method using PEG (poly ethylene glycol) as stabilizer. The prepared samples have been characterized by using X-ray diffraction Spectroscopy (XRD), and Photoluminescence studies (PL). The XRD patterns of the prepared samples represent the tetragonal rutile phase with the particle size of 21-27 nm. The PL Spectra of the undoped samples exhibit emission peaks at 422 nm, 425 nm and 447 nm and co-doped SnO_2 samples also exhibit the same emission peaks with increasing intensity.
Keywords: SnO_2 nanoparticles, PEG, XRD, and PL.

Introduction:

Nanomaterials have attracted a great interest due to their intriguing properties. The fabrication of nanostructure materials has been an active and challenging subject in material science and other fields, because of their unique physical properties and novel potential applications[1-3]. Among II-VI semiconductors, tin oxide (SnO_2) is one of the best host materials for the development of various Optoelectronic devices because of its wide band gap of 3.6eV at room temperature. Tin oxide has a tetragonal structure with point group D^{14}_{4h} and space group P_{42}/mnm; The SnO_2 system with its unique magnetic, optical and electrical properties has generated an enormous interest for its use. In nanostructure SnO_2 a large fraction of atoms on the surface exist in the excited state and thus the electronic property is completely different from that of the bulk. Researchers have been actively investigating this to achieve different morphologies of tin oxide that lead to changes in surface morphology. The surface reactivity changes ultimately affect the electrical, optical, magnetic properties as stated by Shiet et al[4]. The shape of the nanoparticles depends on the reaction conditions during their formation, and many methods such as sol gel[5], hydrothermal[6], and chemical co-precipitation methods[7,8] have been used, Now-a-days many of the researchers have been focusing on alkali, alkaline earth, transition metal and rare earth elements. The microstructure, morphology and luminescence performance of SnO_2 are extremely sensitive to the conditions of their preparation and accordingly lead to many potential applications. In this paper, the changes of SnO_2 nanostructures, photoluminescence, band gap of SnO_2 and morphology induced by Fe (by keeping Al = 5 mol% as constant) are investigated. In the present work pure SnO_2 and $Sn_{1-x}Fe_x Al_yO_2$ (x = 0.00 and 0.01, y = 0.05 as constant) are synthesized and structural, optical properties are investigated.

Synthesis of SnO_2 nanoparticles:

The pristine and co-doped SnO_2 nanoparticles are synthesized by chemical co-precipitation method at room temperature using AR grade stanus chloride dehydrate ($SnCl_2 2H_2O$), sodium hydroxide (NaOH) as precursors, aluminum chloride ($AlCl_3$) and ferrous nitrate ($Fe(NO_3)_2$) as co-doped elements. Initially 0.2 M solution is prepared using Stanus chloride dehydrate and NaOH. For co-doping, ferrous nitrate has been added drop wise to the above solution from 0 to 1 mol% by keeping aluminum chloride as constant at 5 mol%, and added the ammonium solution drop wise under strong stirring until the pH of the solution reaches to 9, and then PEG is added as stabilizer under continuous stirring for 10 hrs. The precipitate is washed repeatedly with de-ionized water to remove impurities formed during the preparation process. After precipitation, the resulting co-doped (Fe, Al) SnO_2 nano powders are dried at 80°C for 12 hrs, then the final precipitate is grinded and annealed at 600 °C for 4 hrs under ambient atmosphere.

Result and Discussion:

Structural Characterization

X-RAY Diffraction:

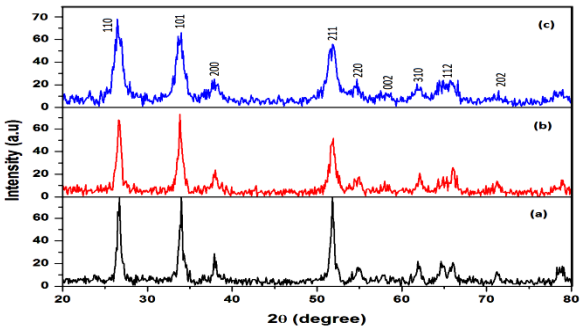

Fig 1. XRD Spectra of (a) Pristine SnO_2 (b) 5 mol% Al doped SnO_2 (c) 1 mol% Fe co-doped SnO_2 nanoparticles.

Fig. 1 represents the XRD pattern of pure and co-doped SnO_2 nanoparticles. The diffraction peaks of the samples correspond to rutile phase of SnO_2 and peak positions are in good agreement with the standard pattern [JCPDS CARD No: 41-1445]. Absence of extra peaks indicates that it has no impurity phases in the samples within the detection limit of the instrument. Co-doped SnO_2 has higher diffracted intensity than pure SnO_2. The crystallite size is calculated by Scherer formula,

$$D = \frac{0.91\lambda}{\beta cos\theta}$$

Here D is the crystallite size, λ is the wavelength of X-rays used and θ is the Braggs angle of diffraction peaks. The estimated particles size for pure and co-doped SnO_2 nanoparticles are 21 nm and 27 nm respectively. The diffraction calculations indicate increase of particle size with A_l doping and Fe co-doping. The ionic radius of Sn^{2+}, Al^{3+} and Fe^{2+} in octahedral co-ordination is 0.69Å, 0.54 Å and 0.64Å respectively. If Al^{3+} and Fe^{2+} substitutes in Sn^{4+} then the lattice should expand as the size of Al^{3+} and Fe^{2+} are larger than that of Sn^{2+}. The expansion in the system due to incorporation of Al^{3+} and Fe^{2+}, can be due to creation of Sn or Oxygen vacancies. However, the formation energy of Sn is lower than that of oxygen[9].

Raman Spectroscopy:

Raman spectroscopy is an effective tool to investigate the vibration modes within the system. A normal mode can be described by the 3n (n is the number of atoms in primitive cell) co-ordinates giving the displacements of atoms from their equilibrium positions[10]. Rutile SnO_2 having six atoms per unit cell gives 18 possible vibrations. On the basis of group theory, the normal lattice vibration, at the point of the Brillion zone can be envisaged[11]. Two modes (A_{2u} and triply degenerate E_u) are infrared (IR) active, A_{2u} has one optic and one acoustic mode.

While E_u has two acoustic, and one optic modes. A_{1g}, B_{1g}, B_{2g} and doubly degenerate E_g are found to be Raman active and A_{2g}, B_{1u} modes are inactive. Chen et al[12] and Lou et al[13] observed IR active peaks in the Raman Spectra. The observed peaks clearly belong to Raman active modes of rutile SnO_2. In bulk SnO_2, Raman active modes are expected at 132, 477, 633, and 778 cm^{-1} from B_{1g}, E_g, A_{1g}, and B_{2g} respectively. In our case, we have clearly observed $A_{1gZ}$and B_{2g} modes. These are respectively due to the expanding and contracting vibrations of Sn-O bonds in a plane perpendicular to c-axis[14]. The E_g mode is accounted for the vibration of two oxygen atoms opposite to each other but parallel to c-axis. This mode is largely sensitive to oxygen vacancies than the other modes[15]. The vibration modes move to higher wave numbers with the co-doped (Fe, Al) SnO_2 and this is due to the crystallite size. With the increase in particle size, confinement of phonon has decreased in small size particles; it leads to the decrease in energy of phonon. These phonons interact with the incident photon such that the scattered photons have lesser energy and thus the peak is shifted to higher wave numbers. Also, the size of the particle increases and broadening of the peaks observed.

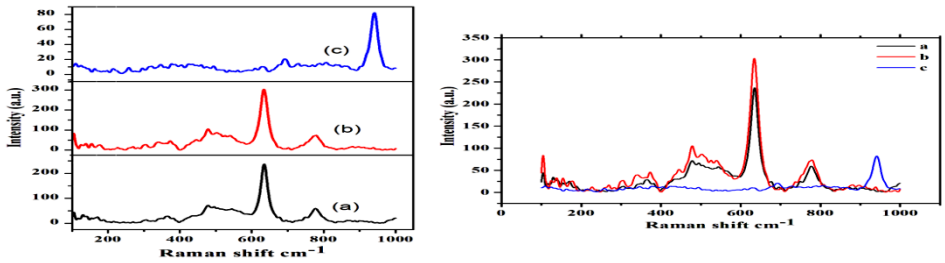

Fig 2. Raman Spectra of (a) pristine SnO_2 (b) 5 mol% Al doped SnO_2 (c) 1 mol% Fe co-doped SnO_2 nanoparticles.

As we co-doped 1 mol% of Fe into 5 mol% of Al doped SnO_2, due to distortion in the system, the intensity of the A_{1g} peak has decreased. The Raman Spectrum is shown in fig.2 In fact, $AlCl_3$, $Fe(NO_3)_2$ have a vibration mode at 633cm^{-1}[16]. The broad peak at 633 cm^{-1} is attributed to A_{1g} non degenerate surface mode. In this mode, oxygen atoms vibrate in the plane perpendicular to the c-axis[17]. When the amount of 1 mol% Fe is co-doped to SnO_2 at constant 5 mol% of Al, Fe-O vibration becomes prominent and starts to contribute to the A_{1g} vibration of Sn-O. The ionic character of the bond between Sn-O is responsible for B_{1g} mode, and increases as Sn^{2+} changes to Sn^{4+}. It means that the bond strength increases as the force constant pushes the peak to higher wave number region. Thus blue shifting in B_{1g} is observed.

FT-IR Spectroscopy Investigations:

FTIR Spectra of all the samples are shown in Fig.3 It is clear from the figure that there are clear changes in the positions, sizes and shapes of IR peaks indicating that co-doped (Fe, Al) might have been incorporated in SnO_2 host. The band exhibited in the low wave number region of 474-620 cm^{-1}, might be due to the vibration of antisymmetric Sn-O-Sn mode of tin oxide, while in the present work SnO_2 band appears in the region 425-515 cm^{-1}. It is also interesting to note that the width of Sn-O-Sn band decreases while O-Sn-O band increases. The observed behavior may be attributed to the improvement in crystalinity due to the removal of residual organic impurities and increase of oxygen content.

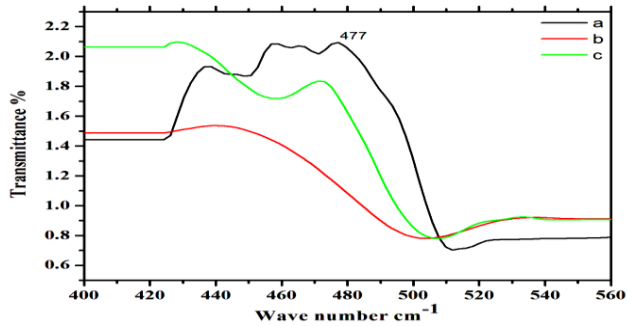

Fig 3. FTIR Spectra of (a) pristine SnO_2 (b) 5 mol% Al doped SnO_2 (c) 1 mol% Fe co-doped SnO_2 nanoparticles.

Further peaks observed in the sample of 1 mol% Fe co-doped around 440 cm^{-1}, 465 cm^{-1}, and 477 cm^{-1} may be due to the IR stretching modes of N-H bonds in NH_4^+. The bands appearing in all the samples around 500 cm^{-1} may be attributed to the bending mode of O-H bonds. Finally, the intensity of broad band appearing in the region 425- 500 cm^{-1} is found to decrease gradually. These observations are in good agreement with previous reports[18]. By comparing FTIR spectra of the samples of the present investigation with those of micro crystalline SnO_2, one may conclude that the position and line shapes of crystalline SnO_2 are different from those of micro crystalline ones.

Optical properties

UV-DRS Spectroscopy :

Fig.4 shows the UV-VIS diffuse reflectance Spectra of pristine, 5 mol% Al doped and 1 mol% Fe co-doped to SnO_2 nano powders annealed at 600° C for 4 hours. The band gap energies calculated using Kubelka-Munk (K-M) model[19] is plotted below.

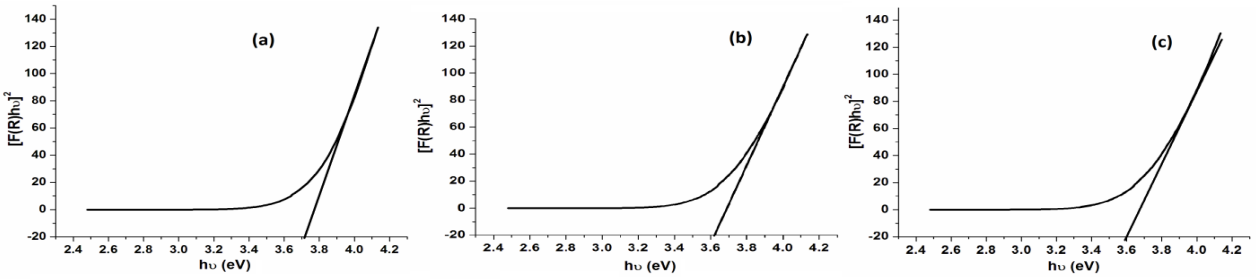

Fig 4. UV-VIS DRS Spectra of (a) pristine SnO_2 (b) 5 mol% Al doped SnO_2 (c) 1 mol% Fe co-doped SnO_2 nanoparticles.

$$\frac{K}{S} = \frac{(1-R_\infty)^2}{2R_\infty} = F(R_\infty) \qquad and \qquad R_\infty = \frac{R\ sample}{R\ standard}$$

The function F (R_∞) is called Kubelka-Munk function, and R is percentage of reflectance[20]. A graph is plotted between [F (R_∞) hυ]^2 vs hυ and the intercept value is the band gap energy[21] of 3.62 eV. It can be seen that the Spectra of co-doped (Fe, Al) SnO_2 shows a considerable blue shift in the band gap transition with co-doping (Fe, Al). The E_g value for pure SnO_2 is 3,6 eV, which is in good agreement with reported values[22]. The co-doped (Fe, Al) SnO_2 exhibit slightly lower band gap. The observed decrease in band gap energy can be attributed to the charge transfer between the Fe, Al ions and SnO_2 conduction or valance bond.

Photoluminescence Spectroscopy:

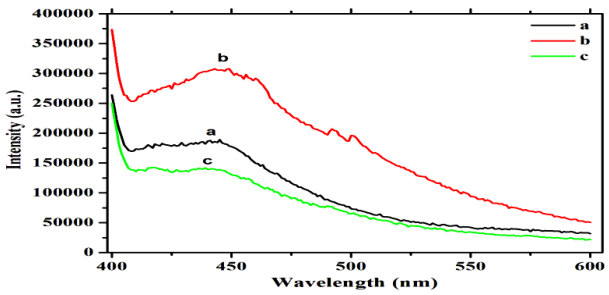

Fig 5. Photoluminescence of (a) pristine SnO_2 (b) 5 mol% Al doped SnO_2 (c) 1 mol% Fe co-doped SnO_2 nanoparticles.

Fig.5 shows the room temperature Photoluminescence Spectra of pristine, 5 mol% Al, and co-doped 1 mol % Fe to SnO_2 nanoparticles. The Spectra show typical UV emission at 422 nm, 429 nm, 447 nm and 490 nm using an excitation wavelength of 350 nm. The 5 mol % Al doped SnO_2 exhibit peaks at 439 nm, 490 nm, 520 nm, and 1 mol % Fe co-doped in SnO2 along with 5 mol % Al shows at 422 nm and 447 nm. The UV

emission in pristine SnO_2 is not due to band edge emission, but due to below band edge emission. The absence of band edge emission may be due to limitations of instrument. The oxygen vacancies can be in three charged states V_o^0, V_o^+ and V_o^{++}, and V_o^0 is the shallowest level while V_o^+ and V_o^{++} are deeper levels within the band gap[23]. In present case, the peak at 422 nm might be due to V_o^0 states, while the peak ranging from 422 nm to 490 nm is due to V_o^+ and V_o^{++} states.

Sharp excitation emission is expected in semiconductors due to multiple luminescence centers. There are various types of surface states that give rise to different energy states inside the semiconductor band gap, for SnO_2. The resulting trapped emission is complicated. The SnO_2 nano crystalline powders have two distinct PL emissions at 439 nm and 486 - 496 nm in the case of the synthesized SnO_2 nanoribbons[24]. Up to now, the mechanisms of observed emissions are not yet clear. However, they should be associated with defect energy levels within the band gap of SnO_2. Oxygen vacancies are well known to be most common defects in oxides and usually act as radioactive center in the luminescence process. Thus, the nature of the transition is tentatively ascribed to Oxygen vacancies, Sn vacancies or Sn interstitials, which form a considerable number of trapped states within the band gap. When SnO_2 nano particles are excited with wave length of 350 nm, Photoluminesent peaks are observed at 425 nm, 490 nm and 520 nm. The visible light emission is known to be related to defect energy levels with the band gap of SnO_2, associated with O vacancies and Sn interstitials[25-28]. In this present work, all the crystalline powders are annealed at 600^0C for 4 hrs and samples have emission peaks observed at 422 nm, 447 nm and 490 nm. The sharp violet emission peak at 447 nm can be ascribed to luminescence centers formed by tin interstials or dangling bonds. However, in the present studies emission maximum at 447 nm, which is lower than the band gap of the bulk SnO_2 of 3.6 eV is observed. These peaks can be attributed to electron transition radiated by defect level in the band gap such as oxygen vacancies and the luminescence centers formed by tin interstials or dangling in the presence of SnO_2 nano crystals. Based on the above discussion, it is concluded that the oxygen vacancies really play an important role in PL from emission spectrum, which is due to the recombination of the electrons with holes in the valance band.

SEM with EDAX:

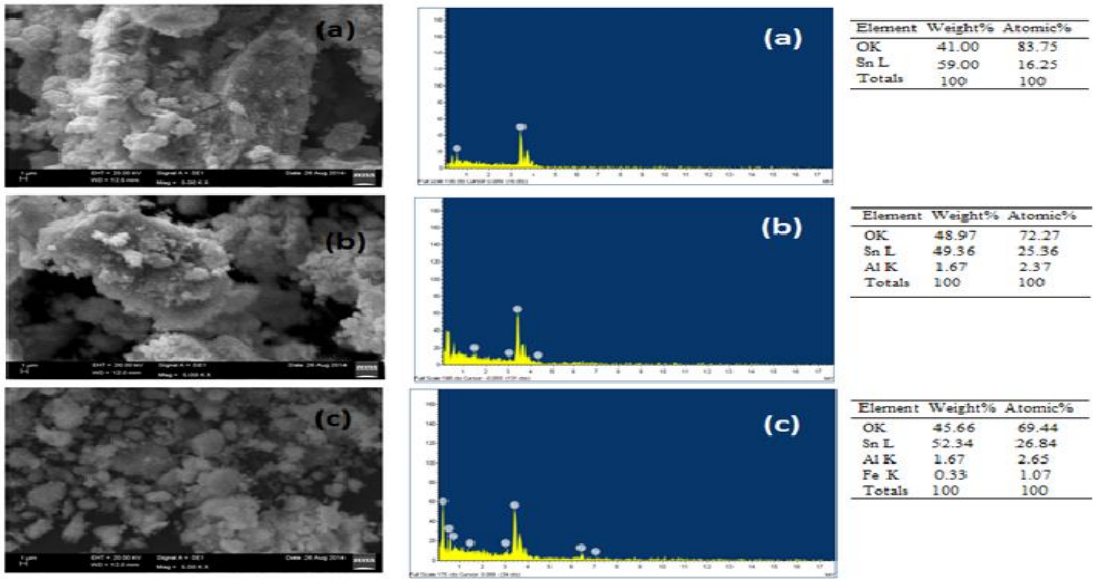

Element	Weight%	Atomic%
OK	41.00	83.75
Sn L	59.00	16.25
Totals	100	100

Element	Weight%	Atomic%
OK	48.97	72.27
Sn L	49.36	25.36
Al K	1.67	2.37
Totals	100	100

Element	Weight%	Atomic%
OK	45.66	69.44
Sn L	52.34	26.84
Al K	1.67	2.65
Fe K	0.33	1.07
Totals	100	100

Fig 6. Micro graphs with EDAX of (a) pristine SnO_2 (b) 5 mol% Al doped SnO_2 (c) 1 mol% Fe co- doped SnO_2 nanoparticles.

From the SEM micrographs, the co-doped (Fe, Al) SnO_2 nano powders morphology is almost spherical in shape and average agglomerate crystal size is estimated to be between 0.2 to 0.3 μm. The agglomeration might be due to strong hydrogen bonding in the precipitate, the agglomerate size increases by co-doping (Fe, Al) to SnO_2. From energy dispersive X-ray Spectrum, chemical compositions is analyzed and the results are in good agreement with standard values mentioned in tables associated with Fig.6

Conclusions:

In summary, tin Oxide (SnO_2) nanocrystalline powders are successfully synthesized by a chemical co-precipitation method in presence of PEG at room temperature. The XRD patterns confirm that SnO_2 nanocrystalline powders possess a tetragonal rutile structure. In the present investigation the crystallite size of the nanoparticles of the co-doped SnO_2 with 1 mol % Fe at 5 mol % of Al is found to be in the range 21-27 nm. The XRD reports are good agreement with the Raman and FTIR analysis. Photoluminescence emission exhibits bands at 422 nm, 447 nm and 490 nm. It is related to the recombination of electrons in singly occupied oxygen vacancies with photo excited holes in the valance band. With co-doped Fe to the 5 mol % of Al to SnO_2, the intensity of peak decreases due to decrease in oxygen vacancies, as revealed by the decrease in luminescence at 460 nm. The diffusion reflectance spectra represent the band gap of pristine, 5 mol % Al and 1 mol % co-doped Fe to SnO_2 and the values are 3.63eV, 3.62eV and 3.6eV respectively. From these values of the band gap of SnO_2 it is evident that there is decrease in band gap by co-doped with Fe, Al. The micrographs from SEM show the spherical shape nanoparticles, and estimated the size of particle is around 0.2 to 0.3μm.

Acknowledgment:

The authors wish to express their gratitude to Prof. Y. Prabhakara Reddy (Retd.), Department of Physics, S.V. University, Tirupati for his help.

References:

1. Lee J.S., Sim S.K., Min B., Cho K., Kim S.W. and Kim S., Structural and optoelectronic properties of SnO_2 nanowires synthesized from ball-milled SnO_2 powders, J. Cryst. Growth, 2004, 267, 145–149.
2. Benshalom A., Kalpan L., Box man R.L., Goldsmith S. and Nasthan M., SnO_2 transparent conductor films produced by filtered vacuum arc deposition, Thin solid films, 1993, 236, 20-26.
3. Choudhury S., Betty C. A., Girija K. G. and Kulshreshtha S. K., Room temperature gas sensitivity of ultrathin SnO_2 films prepared from Langmuir-Blodgett film precursors, Appl. Phys. Lett., 2006, 89, 071914:1-3.
4. Shi L., and Lin H., Preparation of band gap tunable SnO_2 nanotubes and their ethanol sensing properties, 2011, 27, 3977-3981.
5. Nutz T., and Haase M., Wet-chemical synthesis of doped nanoparticles: Optical properties of oxygen-deficient and antimony-doped colloidal SnO_2, J. Phys. Chem., 2000, 104, 8430-8437.
6. Guo C., Cao M., and Hu C., A novel and low-temperature hydrothermal synthesis of SnO_2 nanorods, Inorg. Chem. Commun., 2004, 7, 929-931.
7. Fang, L., Zu, X., Liu, C., Li, Z., Peleckis, G., Zhu, S., Liu, H., and Wang, L., Microstructure and magnetic properties in $Sn_{1-x}Fe_XO_2$ (x=0.01, 0.05, 0.10) nanoparticles synthesized by hydrothermal method, Journal of Alloys and Compounds, 2010, 491, 679-683.
8. Misra S.K., Andronenko S.I., Reddy K.M., Hays J., Thurber A., Punnoose A., A variable temperature Fe^{3+} electron paramagnetic resonance study of $Sn_{1-x}Fe_xO_2$ ($0.00 \leq x \leq 0.05$), J. Appl. Phys. 2007, 101, 09H120:1-3.
9. Van Komen C., Punnoose A. and Seehra M. S., Transition from n-type to p-type destroys ferromagnetism in semi-conducting $Sn_{1-x}Co_xO_2$ and $Sn_{1-x}Cr_xO_2$ nanoparticles, Solid State Communications, 2009, 149, 2257-2259.
10. Zhang K.C., Liu Y., Li Y.F., and Zhu Y., Origin of ferromagnetism in Cu-doped SnO_2: A first-principles study, J. Appl. Phys. 2013. 113, 053713:1-5.
11. Katiyar R. S., Dynamics of the rutile structure. I. Space group representations and the normal mode analysis, J. Phys. C: Solid State Phys, 1970, 3, 1087-1096.
12. Chen W., Ghosh D., and Chen S., Large-scale electrochemical synthesis of SnO_2 nanoparticles, J. Mater. Sci., 2008, 43, 5291-5299.
13. Luo S., Chu P. K., Di Z., Zhang M., Liu W., Lin C., Fan J., Wu X., Vacuum electron field emission from SnO_2 nanowhiskers annealed in N_2 and O_2 atmospheres, Appl. Phys. Lett. 2006, 88,013109-013111.
14. Diéguez, A., Romano-Rodríguez, A., Vilà, A., Morante, J. R., The complete Raman spectrum of nanometric SnO_2 particles, J. Appl. Phys., 2001, 90, 1550-1557.
15. Zhaou W., Liu R., Wan Q., Zhang Q., Pan A.L, Guo .L, and Zou .B, Bound exciton and optical properties of SnO_2 one-dimensional nanostructures, J. Phys. Chem. C, 2009, 113, 1719–1726.

16. Fazio E., Neri F., and Savasta S., Surface-enhanced Raman scattering of SnO_2 bulk material and colloidal solutions, Physical Review B, 2012, 85, 195423:1-7.
17. Xu J.F., Ji W., Shen Z.X., Li W.S., Tang S.H., Ye X.R., Jia D.Z., Xin X.Q., Raman spectra of CuO nanocrystals, J. Raman Spectrosc., 1999, 8, 413–415.
18. Du Y., Zhang M.S., Hong J., Shen Y., Chen Q., Yin Z., Structural and optical properties of nanophase zinc oxide, Appl. Phys. A, 2003, 76, 171-176.
19. Zhu H, Yang D, Yu G, Zhang H and Yao K, A simple hydrothermal route for synthesizing SnO_2 quantum dots, Nanotechnology, 2006, 17, 2386-2389 .
20. Parthibavarman M., Hariharan V., Sekar C., and Singh V.N., Effect of copper on structural, optical and electrochemical properties of SnO_2 nanoparticles, J. Optoele. and Adv. Mat. 12, 2010, 1894 – 1898.
21. Mosadegh Sedghi S., Mortazavi Y., Khodadadi A., Low temperature CO and CH_4 dual selective gas sensor using SnO_2 quantum dots prepared by sonochemical method, Sensors and Actuators B: Chemical, 2010, 145, 7–12.
22. Liu C.M., Zu X.T., Wei Q.M., Wang L.M., Fabrication and characterization of wire-like SnO_2, J. Phys. D, 2006, 39, 2494-2497.
23. Abello L., Bochu B., Gaskov A., Koudryavtseva S., Lucazeau G. and Roumyantseva M., Structural Characterization of Nanocrystalline SnO_2 by X-Ray and Raman Spectroscopy, Journal of Solid State Chemistry, 1998, 135, 78–85.
24. Das S., Kar S. and Chaudhari S., Optical properties of SnO_2 nanoparticles and nanorods synthesized by solvothermal process, J. Appl. Phys., 2006, 99, 114303–114309.
25. Chowdhury P. S., Saha S. and Patra A., Influence of nanoenvironment on luminescence of Eu^{3+}activated SnO_2nanocrystals, Solid State Commun., 2004, 131, 785–788.
26. Kar A, and Patra A, Optical and Electrical properties of Eu^{3+} doped SnO_2 nanocrystals, J. Phys. Chem. C, 2009, 113, 4375-4380.
27. Lee E. J. H., Ribeiro C., Giraldi T.R., Longo E., Leite E.R., Varela J.A., Photoluminescence in quantum-confined SnO_2 nanocrystals: evidence of free exciton decay, Applied Physics Letters, 2004, 84, 1745-1747.
28. Feng Gu, Shu Fen Wang, Meng Kai Lü, Xiu Feng Cheng, Su Wen Liu, Guang Jun Zhou, Dong Xu, Duo Rong Yuan., Luminescence of SnO_2 thin films prepared by spin-coating method, Journal of Crystal Growth, 2004, 262, 182–185.

*****